6. Supplementary Material

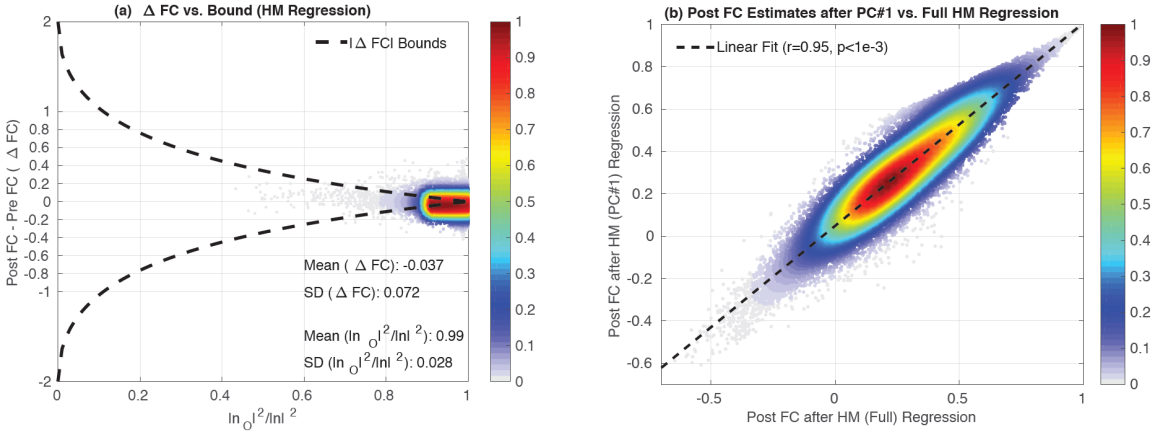

Supplementary Figure 1: (a) Empirical ΔFC values versus orthogonal nuisance fraction $|n_O|^2/|n|^2$ for the 6 HM regressors used in Figure 5a. For this figure full multiple HM regression was performed instead of using the 1$^{\text{st}}$ principal component (PC) of the 6 HM regressors to obtain the ΔFC values, as was performed in the main text. The empirical ΔFC values are clustered around a mean value of -0.04 lie within a fairly narrow neighborhood around the range delineated by theoretical bounds. They do not strictly lie within the bounds because the theoretical framework is currently limited to the case of a single regressor and serves only as a rough guide for multiple regressors. (b) Post FC estimates obtained after regressing out the 1$^{\text{st}}$ PC of HM measurements and estimates obtained after regressing out all 6 HM regressors were strongly correlated with $r = 0.95$.

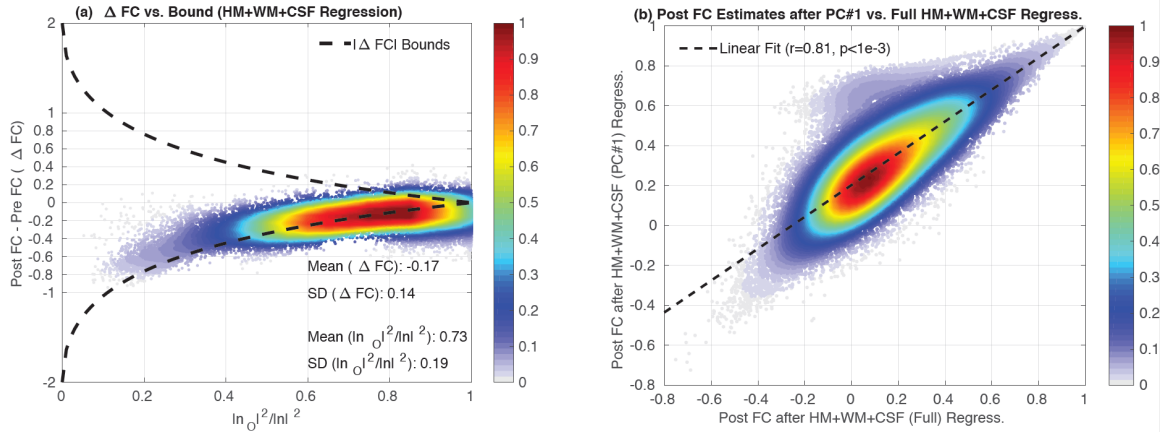

Supplementary Figure 2: (a) Empirical ΔFC values versus the orthogonal nuisance fraction $|n_O|^2/|n|^2$ for the HM+WM+CSF regressors used in Figure 5d. For this example multiple regression was performed instead of using the 1$^{\text{st}}$ principal component (PC) of all the regressors to obtain the ΔFC values, as was performed in the main text. The empirical ΔFC values are clustered around a mean value of -0.17 and lie within a fairly narrow neighborhood around the range delineated by theoretical bounds. They do not strictly lie within the bounds because the theoretical framework is currently limited to the case of a single regressor and serves only as a rough guide for multiple regressors. (b) Post FC estimates obtained after regressing out the 1$^{\text{st}}$ PC of all HM+WM+CSF regressors and after performing multiple HM+WM+CSF regression were strongly correlated with $r = 0.81$.

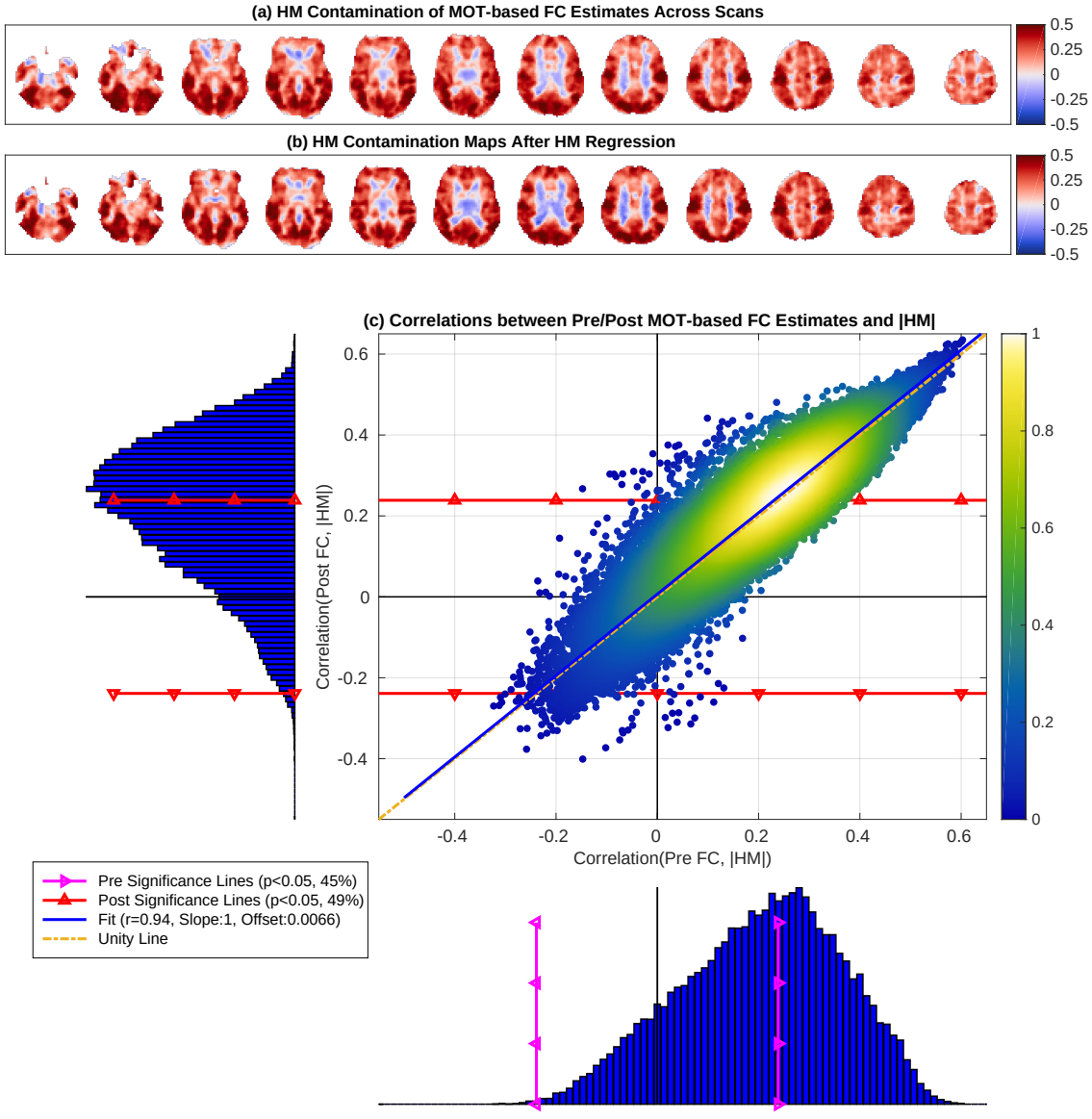

Supplementary Figure 3: MOT-based HM contamination maps (a) before and (b) after HM regression. These maps were fairly similar to each other (cosine similarity $S = 0.98$) and show widespread correlations between the HM norm and FC estimates across scans. The scatter plot in (c) shows the correlations between the Post FC estimates and HM norm after regression versus the correlations obtained between Pre FC estimates and HM norm. These correlation distributions were significantly related ($r = 0.94$, $p < 10^{-3}$) to each other. The linear fit (blue line, Slope= 1 and Offset= 0.007) between the two correlation distributions was nearly identical to the line of unity (dashed yellow line). In the bottom histogram, the correlations between the Pre FC estimates and HM norms ranged from $r = -0.32$ to $r = 0.60$ with mean 0.2, and 45% of these correlations were significant ($p < 0.05$). In the sideways histogram on the left, the correlations between the Post FC estimates and HM norms ranged from $r = -0.40$ to $r = 0.64$ with mean 0.21. The post regression significance lines are shown with red lines with triangles. 49% of the Post FC estimates were significantly correlated with HM norms after regression.

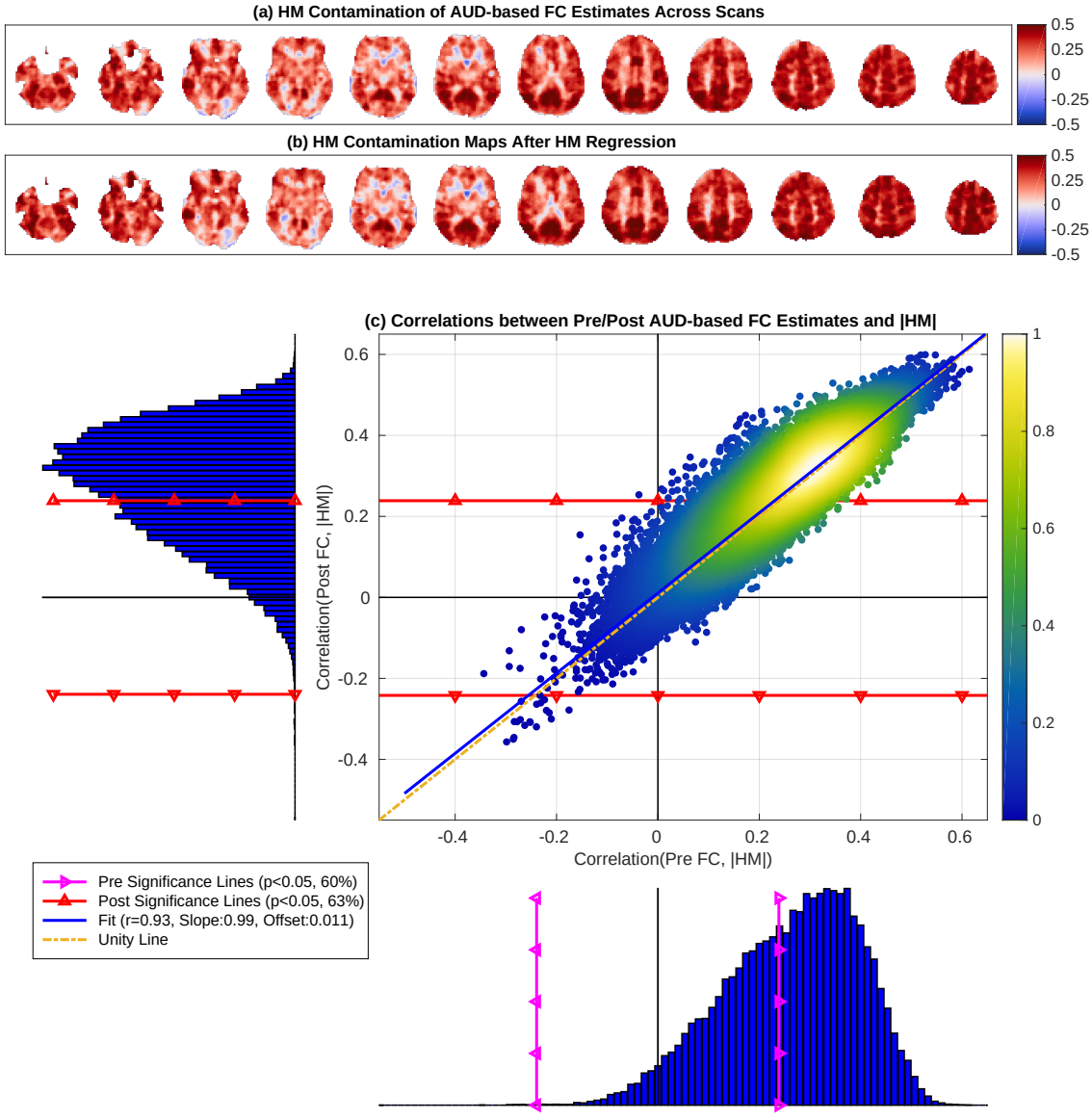

Supplementary Figure 4: AUD-based HM contamination maps (a) before and (b) after HM regression. These maps were fairly similar to each other (cosine similarity $S = 0.99$) and show widespread correlations between the HM norm and FC estimates across scans. The scatter plot in (c) shows the correlations between the Post FC estimates and HM norm after regression versus the correlations obtained between Pre FC estimates and HM norm. These correlation distributions were significantly related ($r = 0.93$, $p < 10^{-3}$) to each other. The linear fit (blue line, Slope= 0.99 and Offset= 0.01) between the two correlation distributions was nearly identical to the line of unity (dashed yellow line). In the bottom histogram, the correlations between the Pre FC estimates and HM norms ranged from $r = -0.34$ to $r = 0.61$ with mean 0.26, and 60% of these correlations were significant ($p < 0.05$). In the sideways histogram on the left, the correlations between the Post FC estimates and HM norms ranged from $r = -0.36$ to $r = 0.60$ with mean 0.27. The post regression significance lines are shown with red lines with triangles. 63% of the Post FC estimates were significantly correlated with HM norms after regression.

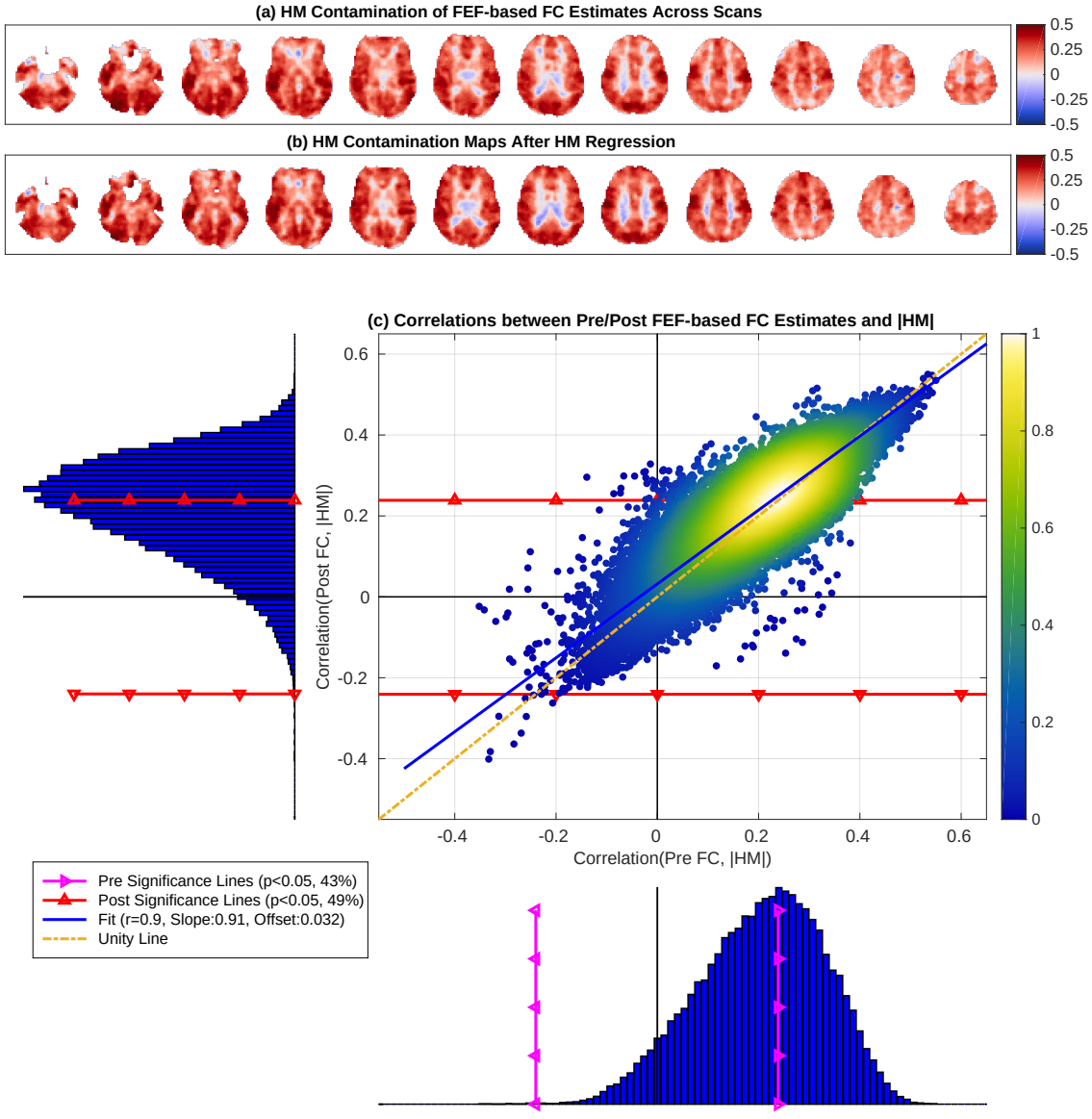

Supplementary Figure 5: FEF-based HM contamination maps (a) before and (b) after HM regression. These maps were fairly similar to each other (cosine similarity $S = 0.97$) and show widespread correlations between the HM norm and FC estimates across scans. The scatter plot in (c) shows the correlations between the Post FC estimates and HM norm after regression versus the correlations obtained between Pre FC estimates and HM norm. These correlation distributions were significantly related ($r = 0.9$, $p < 10^{-3}$) to each other. The linear fit (blue line, Slope= 0.91 and Offset= 0.032) between the two correlation distributions was nearly identical to the line of unity (dashed yellow line). In the bottom histogram, the correlations between the Pre FC estimates and HM norms ranged from $r = -0.34$ to $r = 0.55$ with mean 0.21, and 43% of these correlations were significant ($p < 0.05$). In the sideways histogram on the left, the correlations between the Post FC estimates and HM norms ranged from $r = -0.40$ to $r = 0.55$ with mean 0.22. The post regression significance lines are shown with red lines with triangles. 49% of the Post FC estimates were significantly correlated with HM norms after regression.

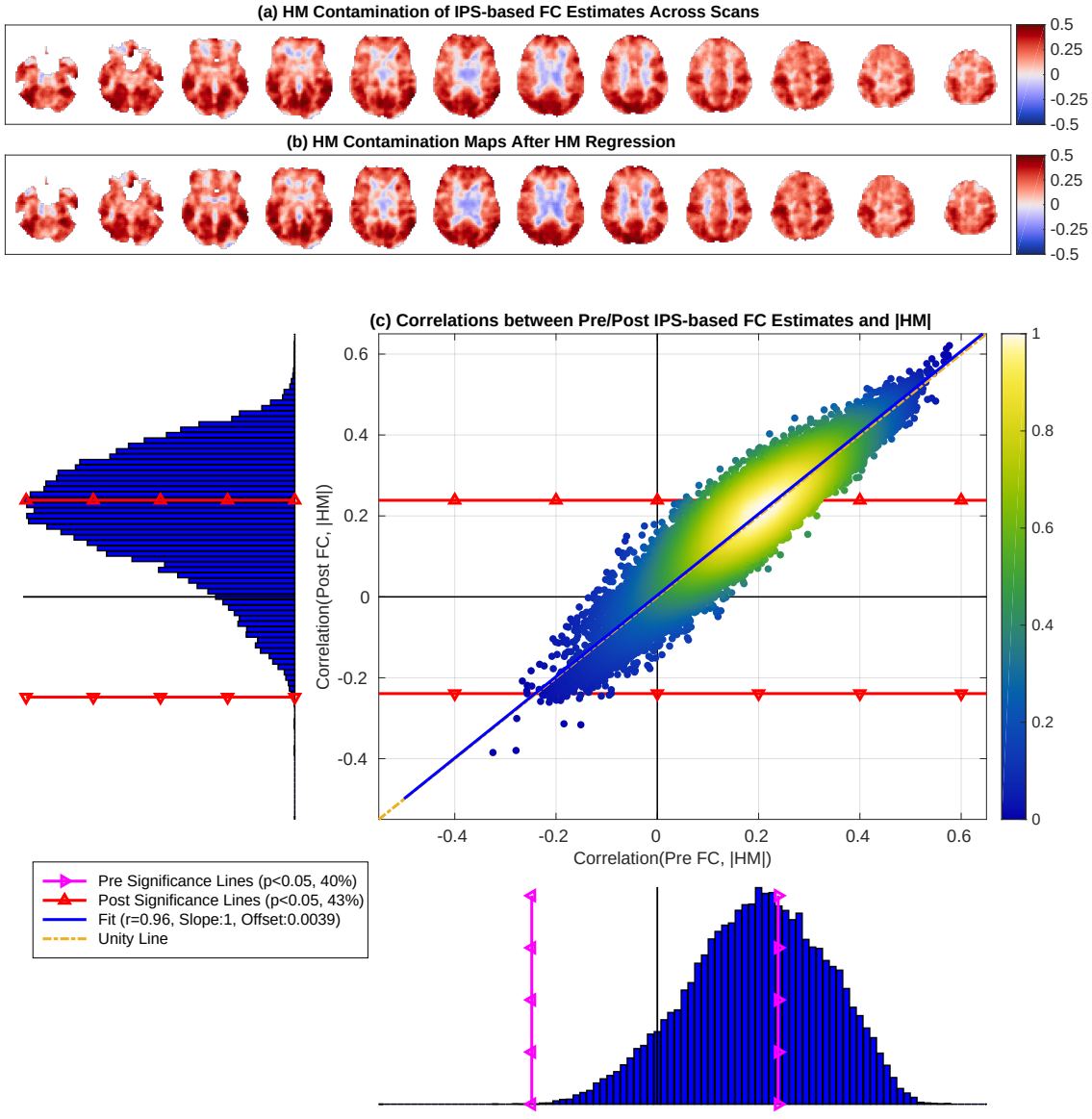

Supplementary Figure 6: IPS-based HM contamination maps (a) before and (b) after HM regression. These maps were fairly similar to each other (cosine similarity $S = 0.99$) and show widespread correlations between the HM norm and FC estimates across scans. The scatter plot in (c) shows the correlations between the Post FC estimates and HM norm after regression versus the correlations obtained between Pre FC estimates and HM norm. These correlation distributions were significantly related ($r = 0.96$, $p < 10^{-3}$) to each other. The linear fit (blue line, Slope= 1.0 and Offset= 0.0039) between the two correlation distributions was nearly identical to the line of unity (dashed yellow line). In the bottom histogram, the correlations between the Pre FC estimates and HM norms ranged from $r = -0.33$ to $r = 0.58$ with mean 0.20, and 40% of these correlations were significant ($p < 0.05$). In the sideways histogram on the left, the correlations between the Post FC estimates and HM norms ranged from $r = -0.36$ to $r = 0.62$ with mean 0.21. The post regression significance lines are shown with red lines with triangles. 43% of the Post FC estimates were significantly correlated with HM norms after regression.

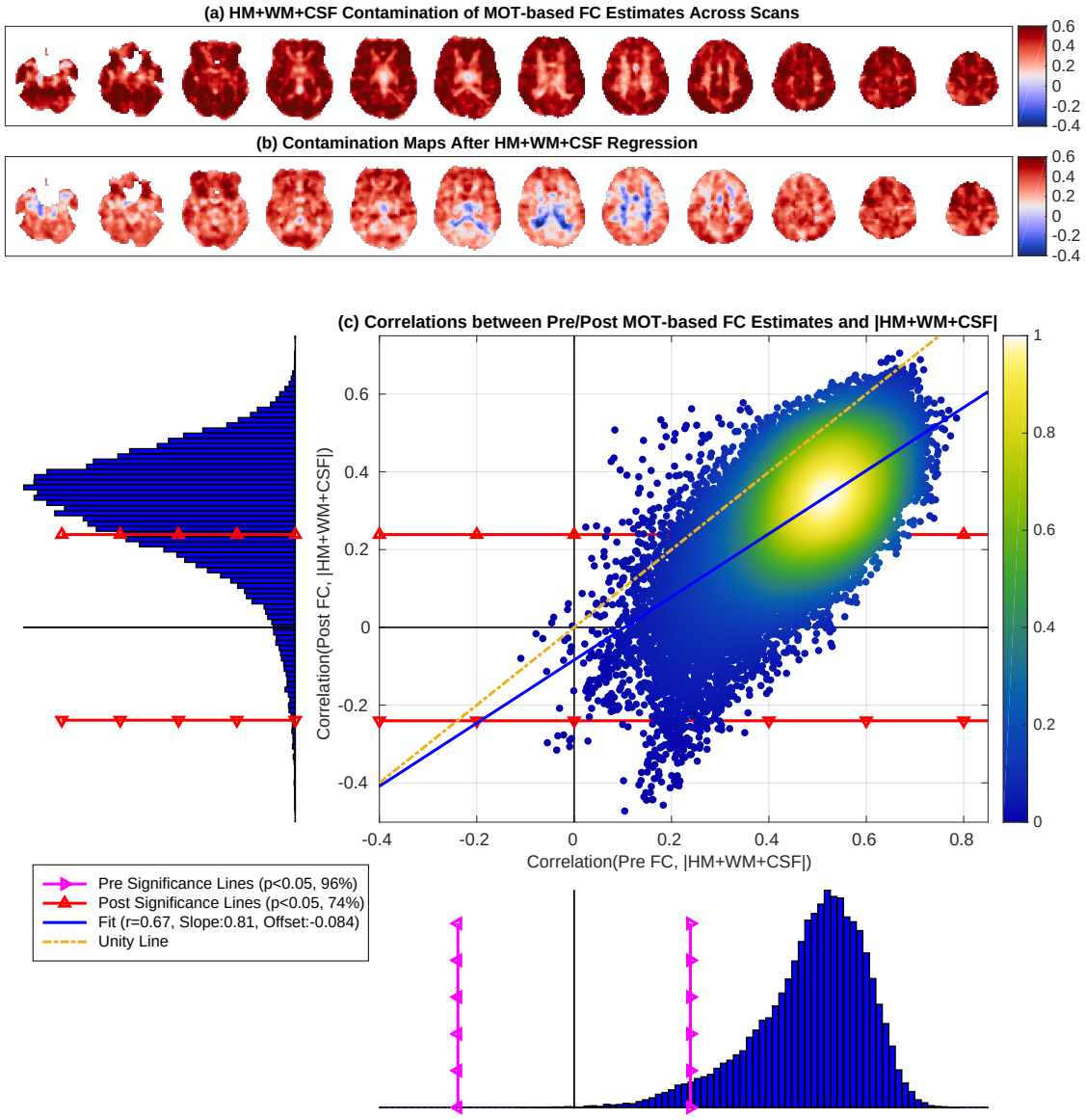

Supplementary Figure 7: MOT-based nuisance contamination maps (a) before and (b) after HM+WM+CSF regression. There was a visible reduction in the correlation values after regression with a slight increase in anti-correlations with blue regions appearing in (b). In (c) the correlations between the Pre FC estimates and the nuisance norm (x-axis) ranged from $r = -0.11$ to $r = 0.76$ with mean 0.49. The correlations between the Post FC estimates and nuisance norm (y-axis) ranged from $r = -0.55$ to $r = 0.71$ with mean 0.31. There was a strong linear relation between the two correlation distributions (linear fit $r = 0.67$, $p < 10^{-3}$). The linear fit between the two correlation distributions was close to the line of unity with a slight reduction in the slope (Slope= 0.81).

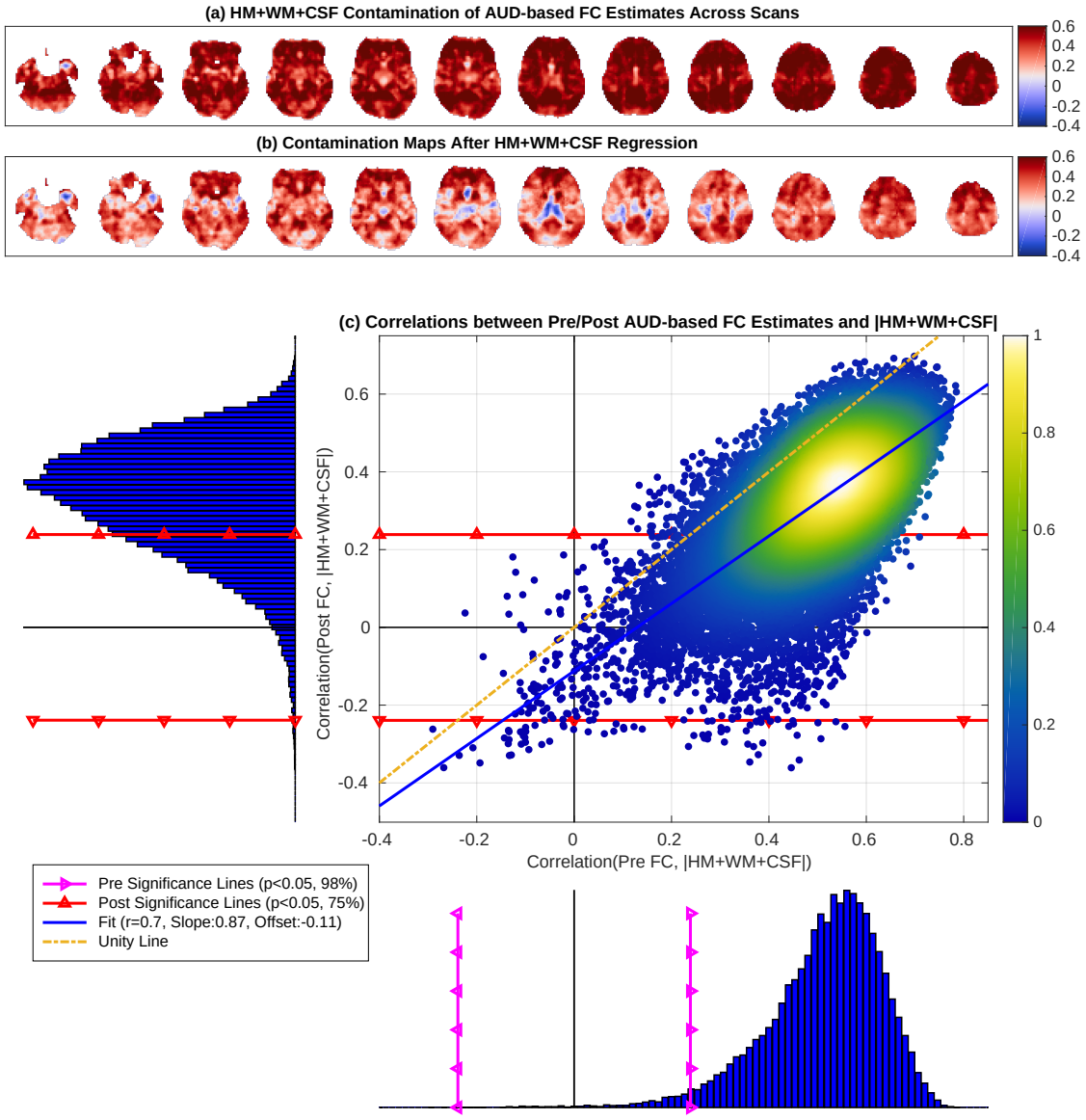

Supplementary Figure 8: AUD-based nuisance contamination maps (a) before and (b) after HM+WM+CSF regression. In (c) the correlations between the Pre FC estimates and the nuisance norm (x-axis) ranged from $r = -0.29$ to $r = 0.79$ with mean 0.51, and 98% of these correlations were significant ($p < 0.05$). The correlations between the Post FC estimates and nuisance norm (y-axis) ranged from $r = -0.36$ to $r = 0.70$ with mean 0.33, and 74% of these correlations were significant ($p < 0.05$). There was a strong linear relation between the two correlation distributions (linear fit $r = 0.70$, $p < 10^{-3}$). The linear fit between the two correlation distributions was close to the line of unity with a slight reduction in the slope (Slope= 0.87) and a small negative offset of -0.11.

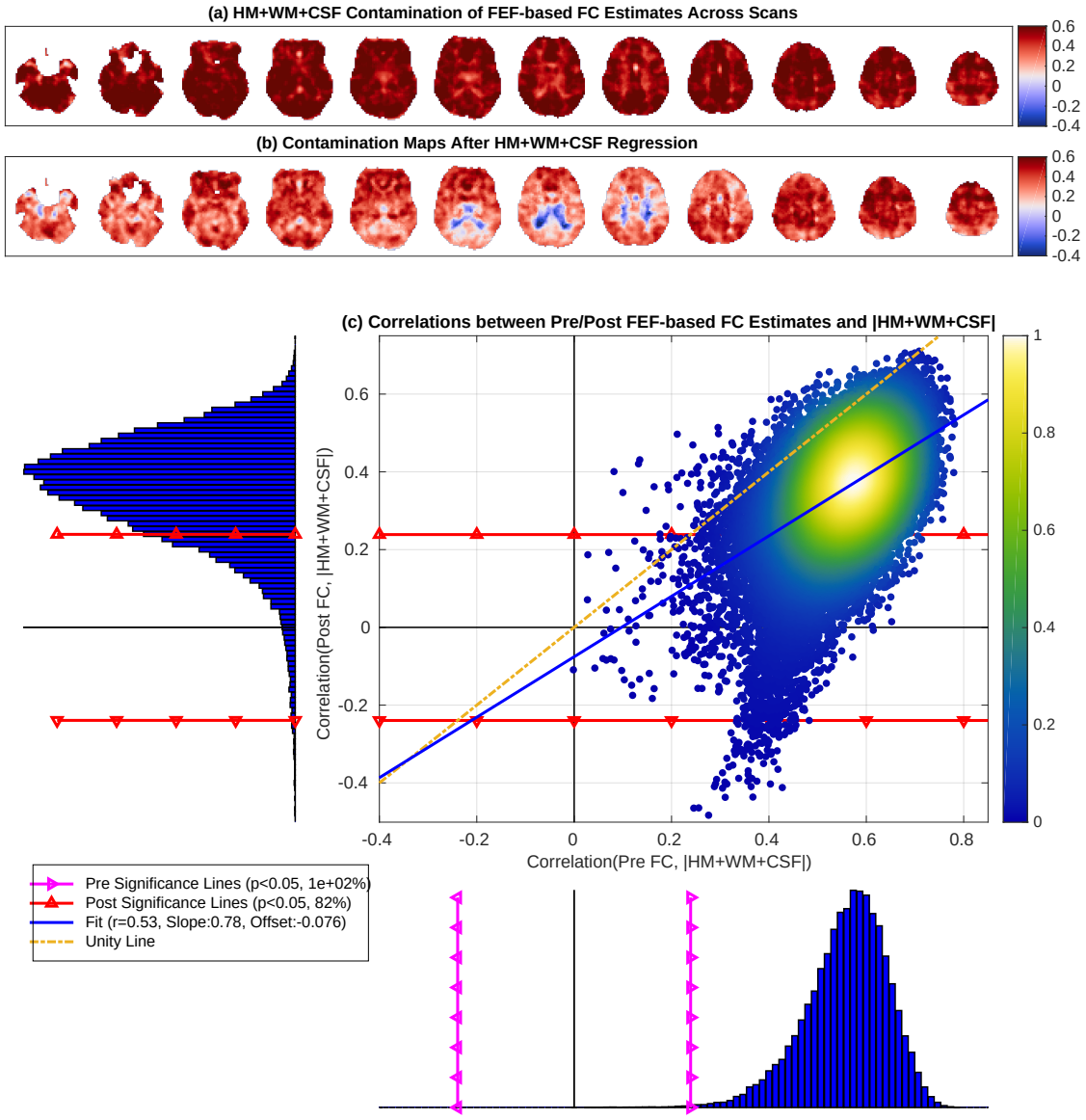

Supplementary Figure 9: FEF-based nuisance contamination maps (a) before and (b) after HM+WM+CSF regression. In (c) the correlations between the Pre FC estimates and the nuisance norm (x-axis) ranged from $r = 0.0$ to $r = 0.78$ with mean 0.56, and 98% of these correlations were significant ($p < 0.05$). The correlations between the Post FC estimates and nuisance norm (y-axis) ranged from $r = -0.51$ to $r = 0.71$ with mean 0.35, and 75% of these correlations were significant ($p < 0.05$). There was a strong linear relation between the two correlation distributions (linear fit $r = 0.53$, $p < 10^{-3}$). The linear fit between the two correlation distributions was close to the line of unity with a slight reduction in the slope (Slope= 0.78) and a small negative offset of -0.08.

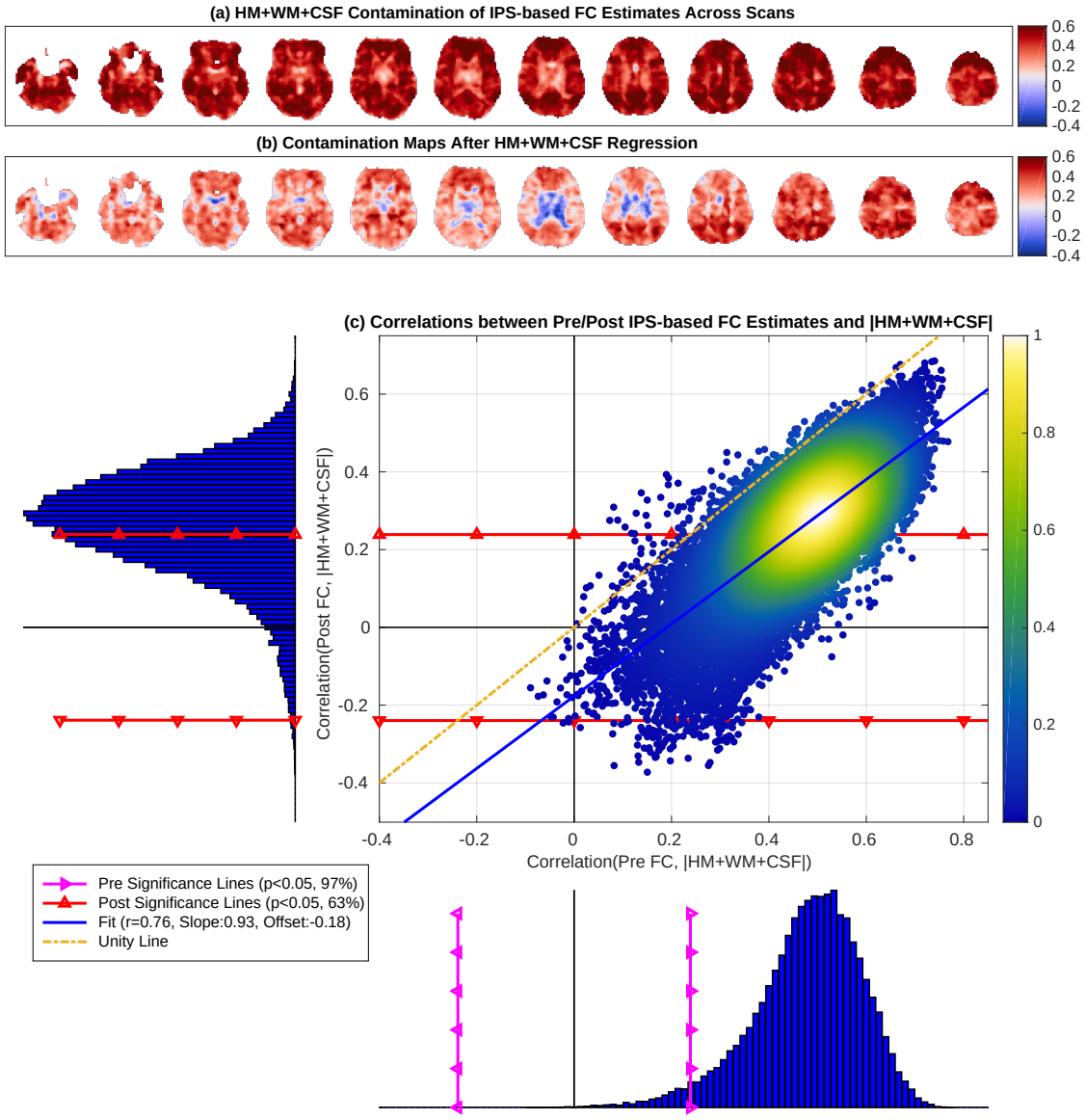

Supplementary Figure 10: IPS-based nuisance contamination maps (a) before and (b) after HM+WM+CSF regression. In (c) the correlations between the Pre FC estimates and the nuisance norm (x-axis) ranged from $r = -0.1$ to $r = 0.77$ with mean 0.48, and 97% of these correlations were significant ($p < 0.05$). The correlations between the Post FC estimates and nuisance norm (y-axis) ranged from $r = -0.37$ to $r = 0.68$ with mean 0.27, and 63% of these correlations were significant ($p < 0.05$). There was a strong linear relation between the two correlation distributions (linear fit $r = 0.76$, $p < 10^{-3}$). The linear fit between the two correlation distributions was close to the line of unity with a slight reduction in the slope (Slope= 0.93) and a small negative offset of -0.18.

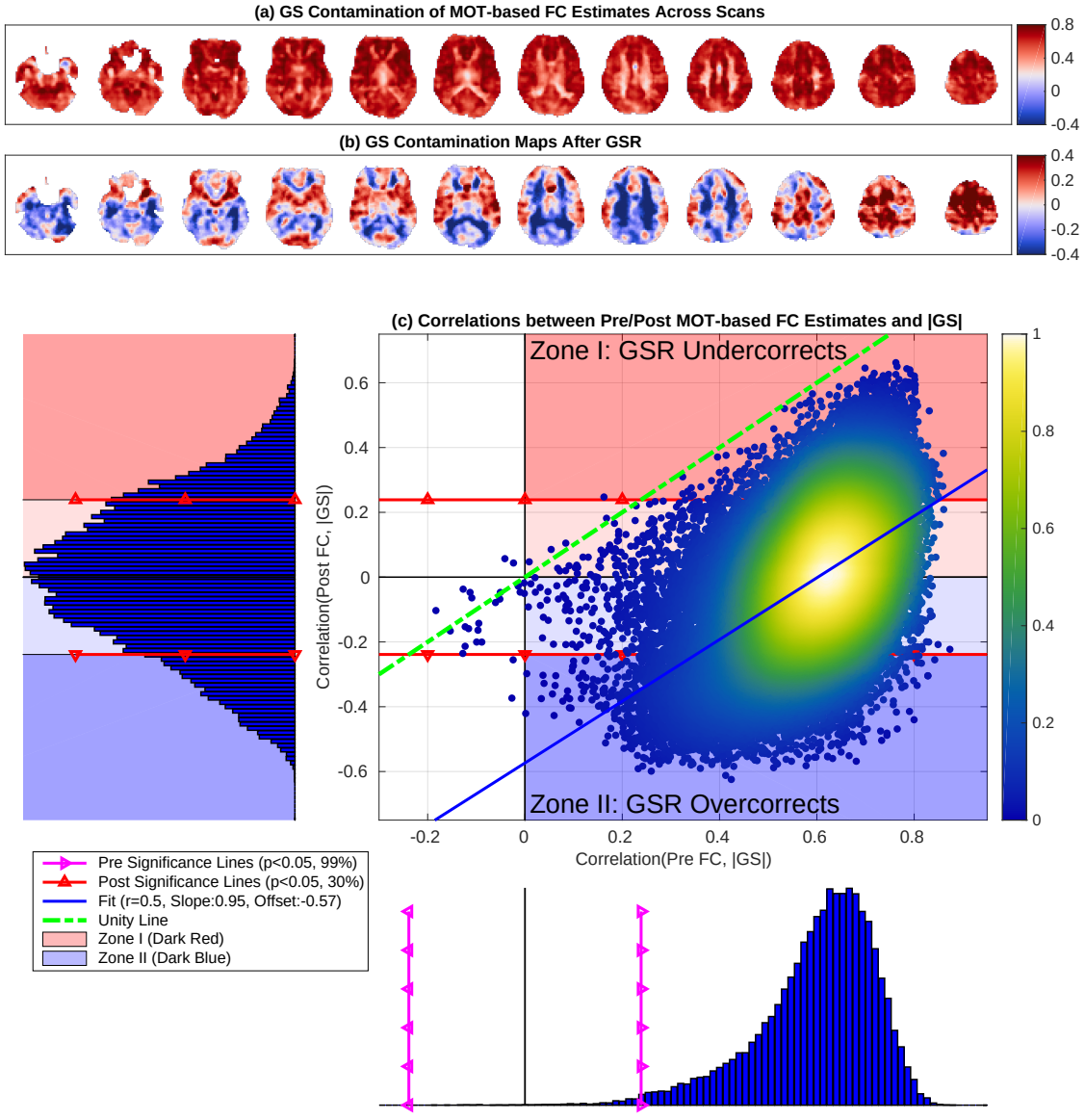

Supplementary Figure 11: MOT-based GS contamination maps obtained both (a) before and (b) after GSR. In panel (a) the contamination map exhibits predominantly positive correlations (99%) between the Pre FC estimates and GS norms. In (b) the contamination map after GSR exhibits both positive (50%) and negative (50%) correlations between the GS norms and Post FC estimates. In (c) the correlations between the Pre FC estimates and the nuisance norm (x-axis) ranged from $r = -0.18$ to $r = 0.87$ with mean 0.60, and 99% of these correlations were significant ($p < 0.05$). The correlations between the Post FC estimates and nuisance norm (y-axis) ranged from $r = -0.62$ to $r = 0.66$ with mean 0.0, and 30% of these correlations were significant ($p < 0.05$). There was a strong linear relation between the two correlation distributions (linear fit $r = 0.50$, $p < 10^{-3}$), and the linear fit (blue line) was fairly parallel to the line of unity with slope of 0.95 and a very large negative offset of -0.57.

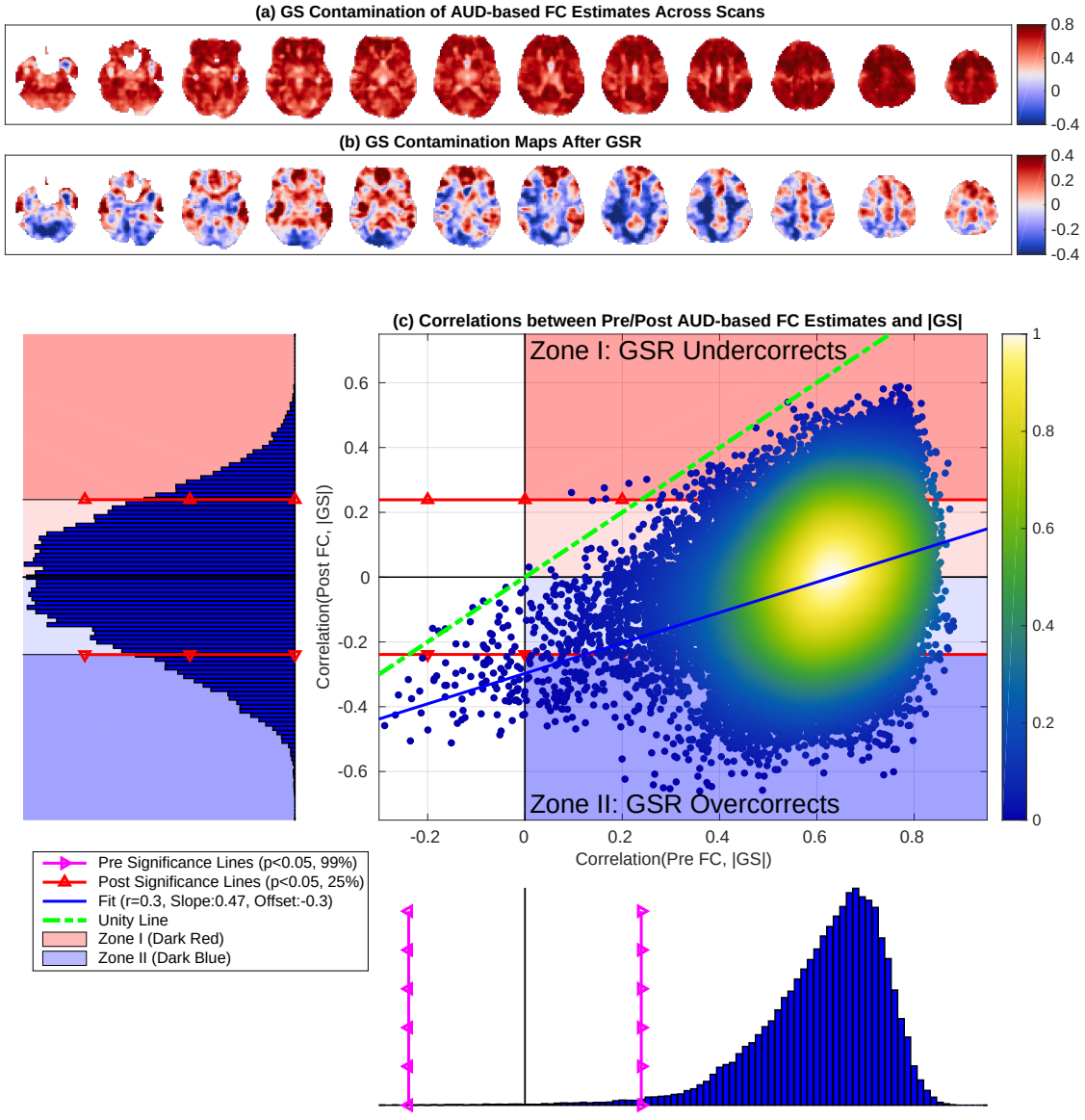

Supplementary Figure 12: AUD-based GS contamination maps obtained both (a) before and (b) after GSR. In panel (a) the contamination map exhibits predominantly positive correlations (99%) between the Pre FC estimates and GS norms. In (b) the contamination map after GSR exhibits both positive (48%) and negative (52%) correlations between the GS norms and Post FC estimates. In (c) the correlations between the Pre FC estimates and the nuisance norm (x-axis) ranged from $r = -0.35$ to $r = 0.88$ with mean 0.61, and 99% of these correlations were significant ($p < 0.05$). The correlations between the Post FC estimates and nuisance norm (y-axis) ranged from $r = -0.66$ to $r = 0.59$ with mean 0.01, and 25% of these correlations were significant ($p < 0.05$). There was a linear relation between the two correlation distributions (linear fit $r = 0.30$, $p < 10^{-3}$), and the linear fit (blue line) was fairly parallel to the line of unity with slope of 0.47 and a large negative offset of -0.30.

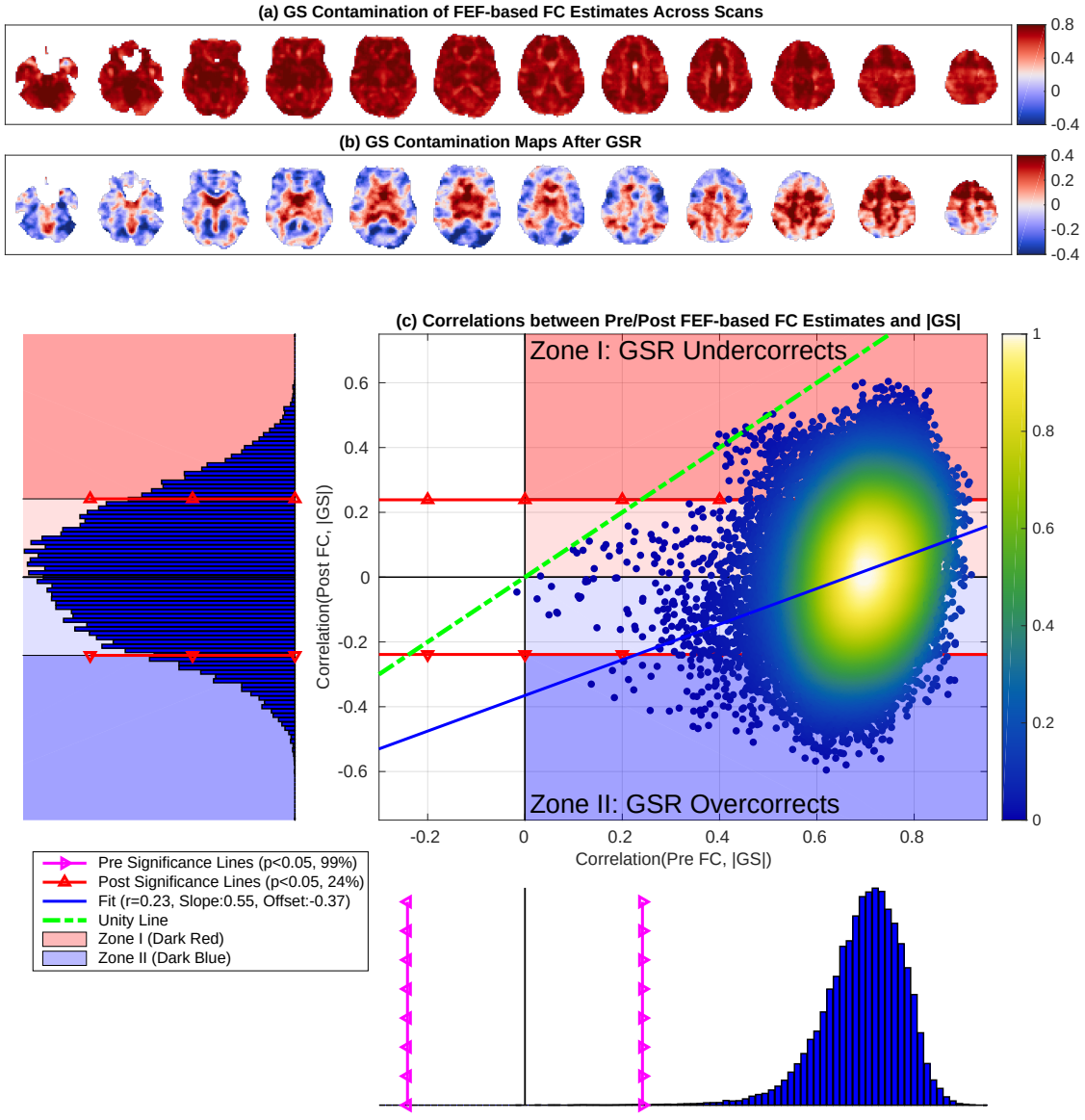

Supplementary Figure 13: FEF-based GS contamination maps obtained both (a) before and (b) after GSR. In panel (a) the contamination map exhibits predominantly positive correlations (100%) between Pre FC estimates and GS norm. In (b) the contamination map after GSR exhibits both positive (53%) and negative (48%) correlations between the GS norms and Post FC estimates. In (c) the correlations between the Pre FC estimates and the nuisance norm (x-axis) ranged from $r = -0.02$ to $r = 0.92$ with mean 0.70, and 100% of these correlations were significant ($p < 0.05$). The correlations between the Post FC estimates and nuisance norm (y-axis) ranged from $r = -0.60$ to $r = 0.60$ with mean 0, and 24% of these correlations were significant ($p < 0.05$). There was a weak linear relation between the two correlation distributions (linear fit $r = 0.23$, $p < 10^{-3}$), and the linear fit (blue line) was moderately parallel to the line of unity with a slope of 0.55 and a large negative offsetof -0.37.

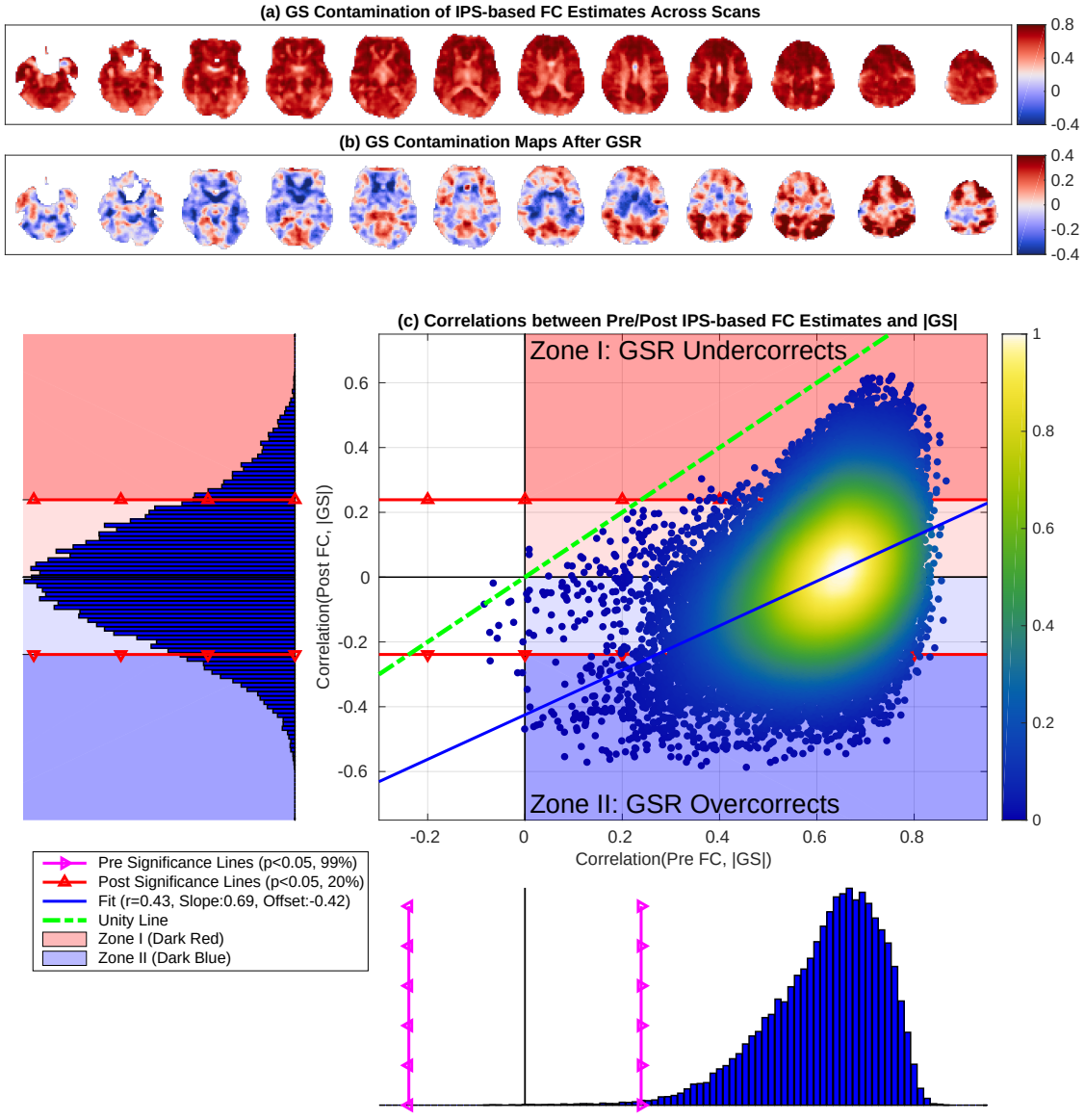

Supplementary Figure 14: IPS-based GS contamination maps obtained both (a) before and (b) after GSR. In panel (a) the contamination map exhibits predominantly positive correlations (100%) between Pre FC estimates and GS norm. In (b) the contamination map after GSR exhibits both positive (49%) and negative (51%) correlations between the GS norms and Post FC estimates. In (c) the correlations between the Pre FC estimates and the nuisance norm (x-axis) ranged from $r = -0.1$ to $r = 0.87$ with mean 0.62, and 100% of these correlations were significant ($p < 0.05$). The correlations between the Post FC estimates and nuisance norm (y-axis) ranged from $r = -0.59$ to $r = 0.62$ with mean 0, and 20% of these correlations were significant ($p < 0.05$). There was a linear relation between the two correlation distributions (linear fit $r = 0.43$, $p < 10^{-3}$), and the linear fit (blue line) was fairly parallel to the line of unity with a slope of 0.69 and a large negative offset of -0.42.

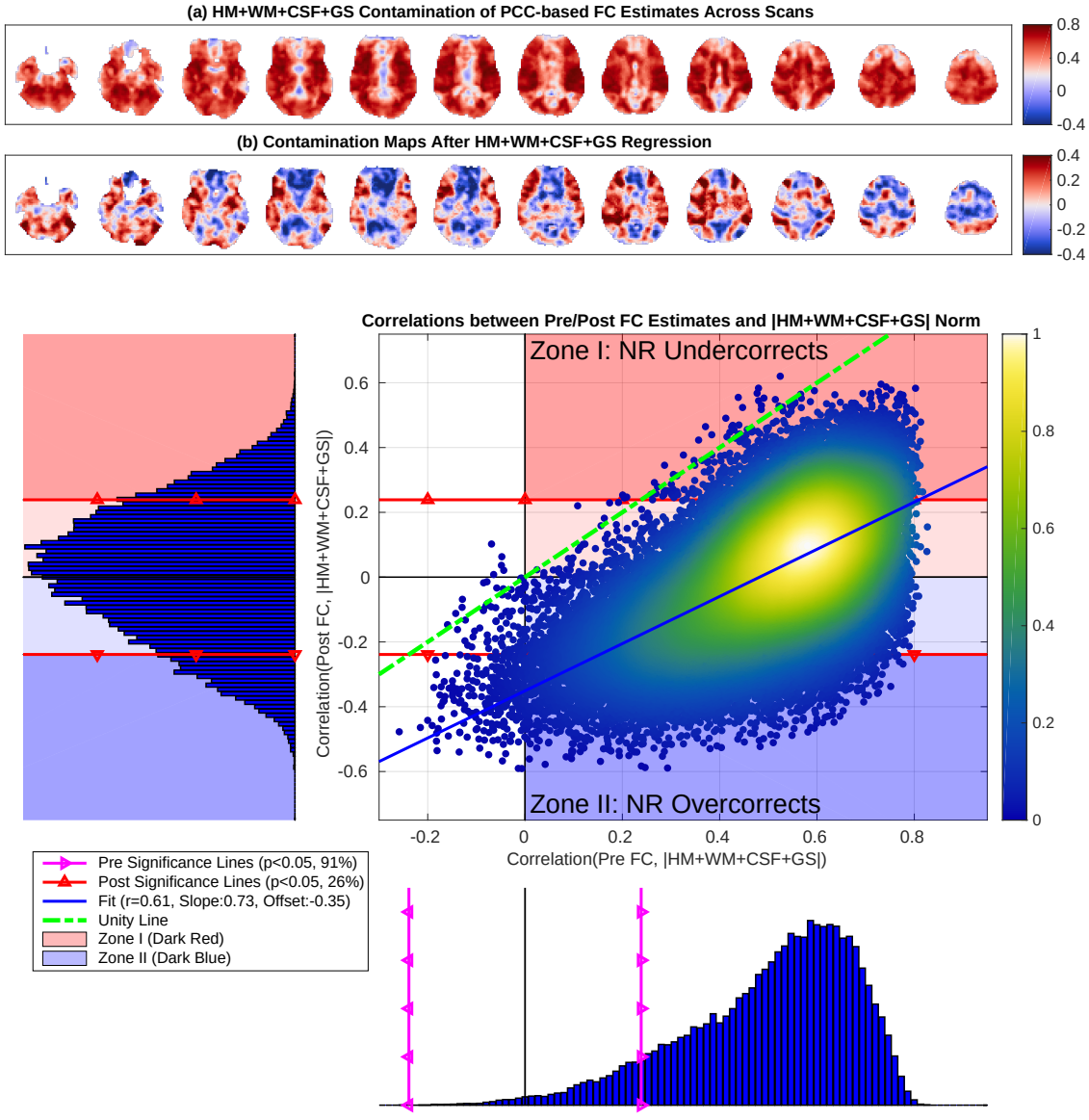

Supplementary Figure 15: PCC-based HM+WM+CSF+GS contamination maps obtained both (a) before and (b) after multiple regression. In panel (a) the contamination map mostly exhibits predominantly positive correlations (99%) between Pre FC estimates and nuisance norm. In (b) the contamination map after nuisance regression exhibits both positive (54%) and negative (46%) correlations between the nuisance norm and Post FC estimates. In (c) the correlations between the Pre FC estimates and the nuisance norm (x-axis) ranged from $r = -0.26$ to $r = 0.83$ with mean 0.50, and 99% of these correlations were significant ($p < 0.05$). The correlations between the Post FC estimates and nuisance norm (y-axis) ranged from $r = -0.59$ to $r = 0.62$ with mean 0.01, and 26% of these correlations were significant ($p < 0.05$). There was a linear relation between the two correlation distributions (linear fit $r = 0.61$, $p < 10^{-3}$), and the linear fit (blue line) was fairly parallel to the line of unity with a slope of 0.73 and a large negative offset of -0.35. These results were very similar to those obtained when performing GSR alone.